Heat and Mass Transfer (2023) 59:2285–2298
https://doi.org/10.1007/s00231-023-03415-2

ORIGINAL ARTICLE

Similarity solutions of a Blasius flow with variable fluid properties and viscous dissipation

Christian Kromer[1] · **Corina Schwitzke**[1] · **Hans-Jörg Bauer**[1]

Received: 25 May 2023 / Accepted: 4 August 2023 / Published online: 16 August 2023

Abstract

An analytical model of the Blasius flow is studied including temperature-dependent fluid properties and viscous dissipation. The friction coefficient and Nusselt number at the wall are calculated from the resulting dimensionless velocity and temperature fields. The variable properties model is compared to a constant properties model to verify if and under which conditions this simplification is valid. Air, water and oil are analyzed as fluids over a representative operating regime, respectively. For air, the variable properties do not influence the friction coefficient and the Nusselt number. For water, the influence of the variable properties is present for both parameters but limited since no large temperature difference can occur in water without a phase change. New correlations for the friction coefficient and Nusselt number were derived for water and oil over a large range of operating conditions. Viscous dissipation does not significantly affect these parameters for air and water because of their relatively low Prandtl numbers. The high Prandtl number of oil in combination with a viscosity that is strongly decreasing with increasing temperature, leads to a more complex behavior. The friction coefficient as well as the Nusselt number are strongly dependent on the fluid properties. Dissipation effects cannot be neglected above an Eckert number of around 0.01. The superposition principle to evaluate wall heat flux in experiments is based on the assumption of constant fluid properties. It can be used without restrictions for air but should be thoroughly checked for all other fluids, especially liquids, using the presented methodology.

Nomenclature: Greek symbols

δ_{99}	Hydrodynamic boundary layer height
δ_T	Temperature boundary layer height
ΔT	Temperature difference
ζ	Relative error
η	Similarity variable
μ	Dynamic viscosity
ν	Kinematic viscosity
ρ	Density
τ	Shear stress
Ψ	Stream function

Latin symbols

c_f	Friction coefficient
c_p	Specific heat at constant pressure
Ec	Eckert number
f	Dimensionless velocity variable
g	Dimensionless temperature
k	Thermal conductivity
Nu	Nusselt number
p	Pressure
Pr	Prandtl number
$\dot{q}$	Heat flux
Re_x	Local film Reynolds number
t	Time
T	Temperature
u	Velocity in x-direction
v	Velocity in y-direction
x	Coordinate parallel to the wall
y	Coordinate normal to the wall

Subscripts and superscripts

film	Average film temperature
w	Wall
aw	Adiabatic wall
∞	Free-stream
$*$	Constant properties model

✉ Christian Kromer
christian.kromer@kit.edu

[1] Institut für Thermische Strömungsmaschinen, Karlsruher Institut für Technologie, Kaiserstr. 12, Karlsruhe 76131, Germany

1 Introduction

The heat transfer from a flow parallel to a flat wall is of complex nature and a function of many parameters such as, e.g. the Reynolds number, the Prandtl number, the Eckert number and the ratios of the fluid properties between wall and free-stream. The reason for the complex relation is the nonlinear character of the Navier-Stokes equations governing the flow and heat transfer. For many applications, the equations can be simplified by assuming constant fluid properties. As a result, the momentum equation uncouples from the energy equation, meaning for example, that a change in wall temperature does not affect the flow field. For a given fluid with known flow boundary conditions, this implies that the wall heat flux is only a function of adiabatic wall temperature and a proportionality constant, namely the heat transfer coefficient: $\dot{q}_w = (T_{aw} - T_w)h$. With this equation, the heat flux for every wall temperature can be obtained. Further neglecting viscous dissipation and any other heat sources or sinks as well as compressibility effects, the adiabatic wall temperature equals the static free-stream temperature and only the heat transfer coefficient needs to be determined. Even when viscous dissipation is included, the linear character of the energy equation for constant fluid properties allows the superposition of several particular solutions. The two parameters, h and T_{aw} have to be determined, e.g. via an experiment, to characterize the heat transfer. Because the adiabatic wall temperature is often difficult to measure experimentally in the presence of a thermal boundary layer, the superposition principle is applied to two heat flux measurements. The two measurements need to have a different wall temperature while not altering the flow [1]. While this approach has been used extensively for air as fluid, e.g. in film cooling [2], there is no clear evidence whether it is a valid approach for other fluids, especially liquids. The present study is, therefore, focused on the flow behavior and heat transfer of a Blasius flow with temperature-dependent fluid properties. The effect of the assumption of constant fluid properties on the fluid flow and heat transfer is evaluated, followed by a discussion whether the superposition method is a valid approach to characterize the heat transfer.

2 Analytical model

The following section starts with an overview of the literature connected to analytical solutions of the Blasius flow with special emphasis to variable fluid properties and viscous dissipation. This is followed by the analytical model of the Blasius flow evaluated in the present study using a similarity solution approach. The section ends with the numerical evaluation and the definition of the target parameters: friction coefficient and Nusselt number.

2.1 Literature review

The fluid flow past a flat plate was first calculated by and subsequently named after Blasius [3]. The governing boundary layer flow equations were solved using a similarity approach. Several authors included variable fluid properties and mainly evaluated an air flow or liquids with Prandtl numbers below 10, such as water [4, 5]. All of these studies neglect the effect of dissipation as it has only a small influence for these fluids and subsonic speeds. However, there has been very little research on high Prandtl number fluids such as oil. Pantokratos is one of the few authors to study oil but also neglecting dissipation [6]. Other studies include the effect of dissipation but neglect the variable fluid properties, such as Korpela [7], Fang [8], Cortell [9] and Olanrewaju et al. [10]. These studies include a wide range of Prandtl numbers from air ($Pr \approx 0.7$) over water up to oil ($Pr > 100$). Only two studies so far include the effect of variable fluid properties and dissipation simultaneously. Mureithi et al. model the viscosity as a function dependent on temperature and use air as their fluid. Khan et al. additionally include the thermal conductivity as a function of temperature, but also use air as their fluid. A list of studies with the corresponding authors and their model properties can be found in Table 1. The studies that included viscous dissipation are indicated by a check mark in the column $Ec \neq 0$. Anderson [11] and Weigand [12] include temperature-dependent fluid properties as well as viscous dissipation in their derivation of the governing equations. Both authors derive the governing dimensionless equations for mass, momentum and energy but do not evaluate them for any fluid or operating conditions.

There is currently no literature available on the superposition principle for high Prandtl number fluids or a large temperature difference between free-stream and wall. Especially the validity of the assumption that temperature-dependent fluid properties do not influence the heat transfer has not been addressed for fluids other than air. However, the simplification of constant fluid properties is necessary in the derivation of the superposition method explained in section 1. The following study focuses, therefore, on the difference between the model with constant and with variable fluid properties. The goal is to identify the operating conditions for different fluids for which the superposition method can be applied. The Blasius flow is chosen in this study, but this can be extended in the future towards Sakiadis flow or to a case where wall and fluid are moving by changing the boundary conditions.

Table 1 Literature on viscous boundary layer flow with heat transfer parallel to a flat surface

ref.	authors	$\rho(T)$	$\mu(T)$	$c_p(T)$	$k(T)$	$Ec \neq 0$
[3]	Blasius	-	-	-	-	-
[4]	Hassanien	√	√	-	√	-
[5]	Bachok et al.	√	√	√	√	-
[6]	Pantokratoras	√	√	√	√	-
[7]	Korpela	-	-	-	-	√
[8]	Fang	-	-	-	-	√
[9]	Cortell	-	-	-	-	√
[10]	Olanrewaju et al.	-	-	-	-	√
[13]	Mureithi et al.	-	√	-	-	√
[14]	Khan et al.	-	√	-	√	√
[11]	Anderson	√	√	√	√	√
[12]	Weigand	√	√	√	√	√

2.2 Derivation

An analytical model of the laminar two-dimensional Blasius flow is used to evaluate the effect of variable fluid properties on the flow and heat transfer behavior. The flow can be described by the Navier-Stokes equations in its stationary form ($\partial/\partial t = 0$). There are no heat sources, no field forces, no radiation and no pressure gradients in x-direction. A schematic of the flow is depicted in Fig. 1. The free-stream with velocity u_∞ and temperature T_∞ flows over a flat plate with temperature T_w. A boundary layer develops over the plate indicated by the dashed line.

The fluid is assumed to be Newtonian with all fluid properties being functions of temperature T. The Navier-Stokes equations are subsequently further simplified by making use of the boundary layer assumptions $u \gg v$ and $\partial/\partial y \gg \partial/\partial x$. u and v are the velocities in x- and y- directions, respectively. The y-momentum equation simplifies to $\partial p/\partial y = 0$, with p being the pressure. This leads to the following set of equations

$$\frac{\partial \rho u}{\partial x} + \frac{\partial \rho v}{\partial y} = 0 \tag{1}$$

$$\rho u \frac{\partial u}{\partial x} + \rho v \frac{\partial u}{\partial y} = \frac{\partial}{\partial y}\left(\mu \frac{\partial u}{\partial y}\right) \tag{2}$$

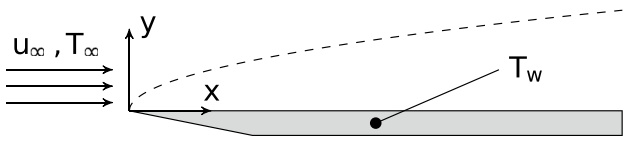

Fig. 1 Schematic of the Blasius flow across a flat surface

$$\rho u c_p \frac{\partial T}{\partial x} + \rho v c_p \frac{\partial T}{\partial y} = \frac{\partial}{\partial y}\left(k \frac{\partial T}{\partial y}\right) + \mu \left(\frac{\partial u}{\partial y}\right)^2 \tag{3}$$

with the density ρ, the dynamic viscosity μ, the specific heat at constant pressure c_p and the thermal conductivity k. The corresponding boundary conditions are $u = v = 0$ and $T = T_w$ at the wall ($y = 0$) and $u \to u_\infty$ and $T \to T_\infty$ outside the boundary layer ($y \to \infty$).

The set of Eqs. (1)–(3) is transformed into a set of dimensionless equations by introducing the similarity parameter $\eta = \sqrt{u_\infty/(\rho_{film}\mu_{film}x)}\int_0^y \rho\, dy$ as the independent variable. The subscript *film* represents the fluid property at film temperature defined as $T_{film} = (T_\infty + T_w)/2$. The dependent variables u and v are replaced by the stream function Ψ, which is defined as $\partial\Psi/\partial y = \rho u$ and $\partial\Psi/\partial x = -\rho v$. The stream function inherently fulfills the mass balance equation and leads to the non-dimensional variable f, defined as $f = \int_0^\eta u/u_\infty d\eta = \Psi/\sqrt{u_\infty \rho_{film}\mu_{film}x}$. The energy equation (Eq. 3) is transformed using the dimensionless temperature $g = (T - T_\infty)/(T_w - T_\infty)$. The coupled equations, with primes denoting differentiation with respect to η, read

$$\left(\frac{\rho}{\rho_{film}}\frac{\mu}{\mu_{film}} f''\right)' + \frac{1}{2} f f'' = 0 \tag{4}$$

$$\left(\frac{\rho}{\rho_{film}}\frac{k}{k_{film}} g'\right)' + \frac{Pr_{film}}{2}\frac{c_p}{c_{p,film}} f g' + Pr_{film} Ec_{film} \frac{\rho}{\rho_{film}}\frac{\mu}{\mu_{film}} \left(f''\right)^2 = 0 \tag{5}$$

with boundary conditions $f = f' = 0$ and $g = 1$ at the wall ($\eta = 0$) and $f' \to 1$ and $g \to 0$ outside the boundary layer ($\eta \to \infty$). $Pr_{film} = \mu_{film} c_p/k_{film}$ denotes the fluid film Prandtl number and $Ec_{film} = u_\infty^2/(c_{p,film}(T_w - T_\infty))$ the fluid film Eckert number. All parameters with subscript "film" indicate

that the respective fluid properties are evaluated at fluid film temperature.

2.3 Evaluation

The set of nonlinear ordinary differential equations (ODE) of higher order is transformed into a set of first order ODEs and subsequently solved with the *odeint* package in Python. The *odeint* package is part of the open-source environment *scipy* (v.1.10.1), used to analyze data with tools like optimization, integration or solving differential equations. The relative tolerance of the variables in the numerical evaluation is set to 10^{-8} and the absolute tolerance to 10^{-10}. The solver controls the estimated local error and stops once it falls below the sum of the relative tolerance times the result and the absolute tolerance. The independent variable η is discretized in the range [0, 30] with a step size of 0.01. All these settings are kept constant during all simulations.l The value of $\eta = 30$ is chosen to ensure that the upper limit of the computational domain has no influence on the simulation results as previously mentioned by Andersson and Aarseth [15]. The boundary value problem is solved as an initial value problem using the shooting method [11]. Only three initial values are given and two boundary conditions at $\eta \to \infty$. The two missing starting conditions are iteratively determined until the boundary conditions for the free-stream are satisfied and the threshold of the relative error is smaller than 10^{-5} at $\eta = 30$. The numerical solution for f and g and their derivatives represent the velocity and the temperature field inside the boundary layer of the Blasius flow.

The dimensionless numbers friction coefficient c_f and Nusselt number Nu are subsequently evaluated with the help of the calculated flow field variables f and g

$$c_\mathrm{f} = \frac{2\tau_\mathrm{w}}{\rho_\infty u_\infty^2} = \frac{2}{\sqrt{Re_x}} \frac{\rho_\mathrm{w}}{\rho_\infty} \frac{\mu_\mathrm{w}}{\mu_\mathrm{film}} f''(0) \tag{6}$$

$$\begin{aligned} Nu &= \frac{\dot{q}_\mathrm{w} x}{k_\mathrm{film}\left(T_\mathrm{w} - T_\mathrm{aw}\right)} \\ &= -\sqrt{Re_x} \frac{T_\mathrm{w} - T_\infty}{T_\mathrm{w} - T_\mathrm{aw}} \frac{\rho_\mathrm{w}}{\rho_\mathrm{film}} \frac{k_\mathrm{w}}{k_\mathrm{film}} g'(0) \end{aligned} \tag{7}$$

with the local film Reynolds number $Re_x = \rho_\mathrm{film} u_\infty x / \mu_\mathrm{film}$ and the adiabatic wall temperature T_aw. An additional calculation is necessary because the driving temperature difference $T_\mathrm{w} - T_\mathrm{aw}$ is still unknown. The governing equations (Eqs. 4 and 5) are solved a second time with the additional boundary condition $g'(0) = 0$, representing an adiabatic wall. The temperature of the wall, however, is unknown a priori, which is why it is one of the variables to be solved for iteratively.

Subsequently, a comparison is drawn between the results of a constant fluid properties model to the already described variable fluid properties model. The constant fluid properties model is represented by the same governing equations (Eqs. 4 and 5), boundary conditions and evaluation parameters (Eqs. 6 and 7). Any derivatives of fluid properties equal zero and all fractions involving fluid properties simplify to one. The only exception is the evaluation of the friction coefficient, where a fraction of $\rho_\mathrm{film}/\rho_\infty$ remains. The model uses the constant film density, but the definition of the friction coefficient calls for the free-stream density, leading to the aforementioned term. The relative error ζ is deduced for the friction coefficient and the Nusselt number as

$$\zeta_{c_\mathrm{f}} = \frac{c_\mathrm{f}^* - c_\mathrm{f}}{c_\mathrm{f}} \tag{8}$$

$$\zeta_{Nu} = \frac{Nu^* - Nu}{Nu} \tag{9}$$

with the constant fluid properties model indicated by the index *. A value of zero indicates a perfect match between the constant and variable properties models. A positive value indicates an overestimation and a negative value an underestimation by the constant properties model with the variable properties model as the reference.

3 Results

The fluids investigated in this study are air, water and Mobil jet oil II, a typical oil for aeroengine applications. Their fluid properties are evaluated with the equations by Zografos et al. [16] for air and water and by Glahn [17] for oil. These fluids are chosen instead of simply varying the dimensionless parameters because the fluid properties as well as the Prandtl number cannot be chosen randomly since they are connected via the temperature. The results of the numerical evaluations of Eqs. (4) and (5) are presented in dimensionless form wherever possible. The variable fluid properties, however, introduce several dimensionless products, such as $\rho_\mathrm{w}/\rho_\mathrm{film}$, that cannot be changed independently of each other. The fluid properties as well as the Prandtl number are all solely functions of temperature, and all change according to the fluid property equations. Hence, the film temperature and the temperature difference $\Delta T = T_\mathrm{w} - T_\infty$ are varied to minimize the input parameters.

3.1 Velocity and temperature profiles

The boundary layer profiles for oil at $T_\mathrm{film} = 323.15\mathrm{K}$ and $\Delta T = 0.1\mathrm{K}$ are investigated. Those temperature values are chosen to eliminate the variable fluid properties

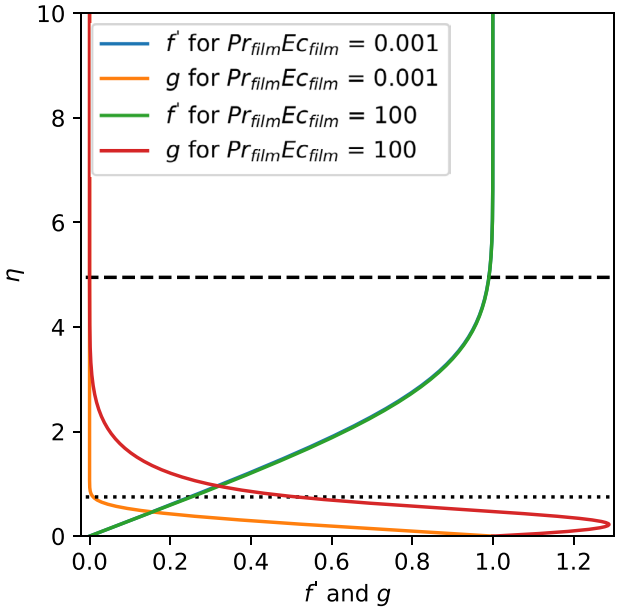

Fig. 2 Velocity (f') and temperature (g) profiles across the boundary layer for oil with $Pr_{\text{film}} = 244$. The first case has no dissipation, where $Pr_{\text{film}}\, Ec_{\text{film}} = 0.001$ (blue and orange lines) and the second case has significant dissipation with $Pr_{\text{film}}\, Ec_{\text{film}} = 100$ (green and red lines). The blue line coincides with the green line and is therefore not visible. For the first case without dissipation, dashed and dotted lines are added to indicate the velocity boundary layer height of $\eta = 4.91$ and the temperature boundary layer height of $\eta = 0.72$, respectively

and to maximize the Prandtl number of the flow, in this case $Pr_{\text{film}} = 244$. Two different flow velocities are investigated such that the dissipation term is either negligible ($Pr_{\text{film}}\, Ec_{\text{film}} = 0.001$) or exhibits significant influence on the temperature profile ($Pr_{\text{film}}\, Ec_{\text{film}} = 100$).

In Fig. 2, the dimensionless velocity f' and temperature g profiles are plotted for both dissipation cases versus the similarity parameter η. The velocity profiles for both cases coincide since the temperature difference ΔT is so small that the fluid properties are close to constant. The temperature profiles, however, differ significantly inside the thermal boundary layer. In the case of large dissipation, an increase in temperature above the wall temperature can be noticed inside the thermal boundary layer. This means, that the wall is heated by the flow through dissipation even though the free-stream temperature is below the wall temperature. For the case without dissipation, the dashed and dotted lines indicate the boundary of the velocity and temperature boundary layer height, respectively. The hydrodynamic boundary layer height δ_{99} is defined as the distance normal to the wall at which the velocity reaches 99% of the free-stream velocity. The thermal boundary layer height δ_T is defined similarly with the temperature equaling $T_{\text{w}} + 0.99\left(T_{\infty} - T_{\text{w}}\right)$. The ratio of boundary layer heights $\delta_T/\delta_{99} = 0.74/4.91 = 0.151$ is in good accordance with literature on laminar boundary layers [18], which approximates this ratio to

$$\frac{\delta_T}{\delta_{99}} \approx \left(\frac{14}{13} Pr_{\text{film}}\right)^{-\frac{1}{3}} = 0.156\,. \tag{10}$$

The difference between the two values is probably due to the approximation in the derivation in the literature.

The influence of variable fluid properties on the boundary layer heights is depicted in Fig. 3. The constant properties model exhibits a constant behavior at the values presented above. The variable properties model, however, shows a strong positive correlation for the hydrodynamic and a slight negative correlation for the thermal boundary layer with respect to the temperature difference. Regarding the flow, the change in viscosity is the main reason for the change in boundary layer height. As explained above,

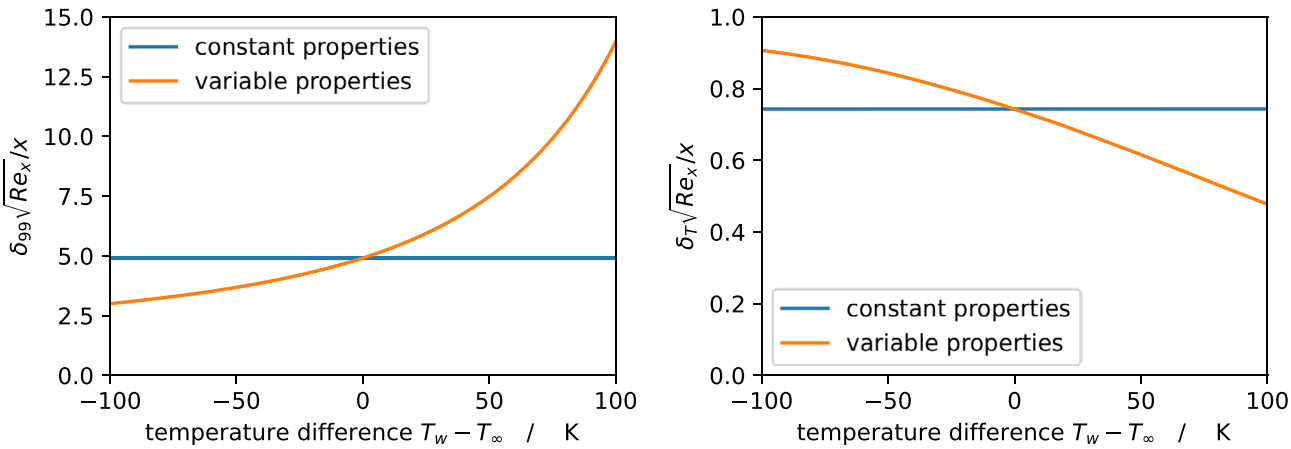

Fig. 3 Hydrodynamic (left) and thermal (right) boundary layer height over temperature difference for oil at $Pr_{\text{film}} = 244$ without dissipation. The results for variable and constant fluid properties are plotted in blue and orange, respectively

the thermal boundary layer is much smaller than the hydrodynamic one. Therefore, almost the entire hydrodynamic boundary layer is at the free-stream temperature. The Reynolds number based on the film temperature Re_x does not fully account for the influence of the viscosity, leading to the increase in boundary layer height on the left hand side of Fig. 3. The change in thermal boundary layer height is the result of the varying velocity profile. For large negative temperature differences, a thin highly viscous layer forms along the wall that is barely moving. Such a layer decreases the heat transfer at the wall and subsequently increases the thermal boundary layer. The opposite effect occurs for positive temperature differences, where a thin layer of little viscosity increases the velocity gradient. Consequently, the convective heat transfer is enhanced and the boundary layer height decreases.

3.2 Friction coefficient and Nusselt number

The temperature difference is varied to investigate the influence of the fluid properties on the flow and heat transfer behavior. The friction coefficient and the Nusselt number are evaluated for oil at $Pr_{\text{film}} = 244$ and $Pr_{\text{film}}\,|Ec_{\text{film}}| = 0.001$. The latter value is chosen to exclude any dissipation effects and the absolute value of the Eckert number to obtain only positive numbers, since the temperature difference is negative once the free-stream is hotter than the wall.

The friction coefficient multiplied by the square root of the local Reynolds number is plotted on the left in Fig. 4 for the variable and constant fluid properties models in blue and orange, respectively. The constant properties model shows a slight decrease, while the variable properties model shows a strong positive correlation with the input parameter ΔT. The behavior of the constant properties model can be explained by the momentum equation being decoupled from the temperature field, leading to a constant solution for $f''(0)$. However, the density used in the model is the film density ρ_{film} while the definition of the friction coefficient uses the free-stream density ρ_∞. The remaining fraction $\rho_{\text{film}}/\rho_\infty$ leads to the slight decrease of the friction coefficient. The behavior of the variable properties model is mainly driven by the temperature dependence of the viscosity. A positive temperature difference (cold free-stream over hot wall) leads to a thin thermal boundary layer of low viscosity underneath a thick momentum boundary layer of high viscosity. The viscosity at the wall decreases more by a factor of around 4 going from $\Delta T = 1$K to 100 K. However, the velocity gradient at the wall is increasing simultaneously by a factor of around 10, leading to an overall increase of the friction coefficient. For negative temperature differences, the same reasoning explains the decrease of the friction coefficient for the variable properties model.

A similar trend as for the friction coefficient is shown on the right hand side in Fig. 4 for the heat transfer, represented by the Nusselt number divided by the square root of the local Reynolds number. As long as no dissipation is present and the fluid properties are constant, the Nusselt number is independent of the temperature difference. The variable properties model exhibits a positive correlation with the temperature difference. The main reason for this behavior is the significant change in the velocity profile with increasing ΔT explained in the previous paragraph. The changes in density, thermal conductivity and specific heat with varying temperature difference are rather small compared to the changes in viscosity and can be neglected.

3.3 Variable properties and Prandtl number

With the boundary layer profiles and the influence of the temperature difference established, the focus shifts to the

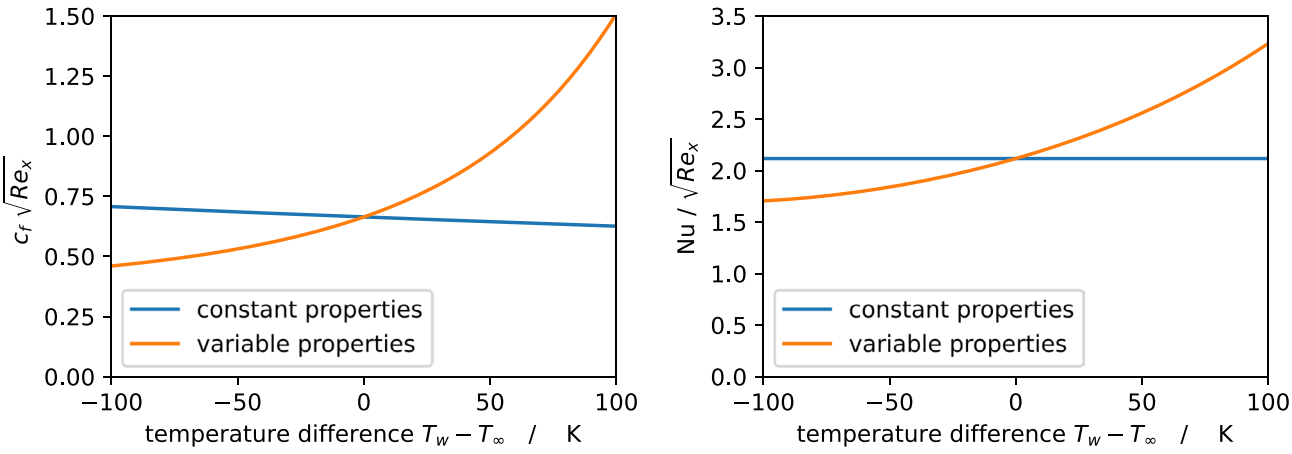

Fig. 4 Friction coefficient (left) and Nusselt number (right) over temperature difference for oil at $Pr_{\text{film}} = 244$ and without dissipation. The results for variable and constant fluid properties are plotted in blue and orange, respectively

applicability of the constant properties model for a large range of operating conditions. The relative errors ζ_{c_f} and ζ_{Nu} as defined by Eqs. (8) and (9) are evaluated for a large range of film temperatures and temperature differences. The constant properties model is deemed to be a very good approximation for relative errors below 1% and a reasonably good approximation for $\zeta < 10\%$. This is why the error values are highlighted by dotted and dashed lines hereafter in all plots. The product $Pr_{\text{film}} |Ec_{\text{film}}|$ is again kept constant at 0.001 to be able to neglect dissipation. All three investigated fluids (air, water and oil) are simulated with their respective fluid properties to elaborate on fluids with largely different Prandtl numbers.

3.3.1 Air

Figure 5 depicts the relative error for the friction coefficient (left) and for the Nusselt number (right) for air. There are no significant differences for the friction coefficient and the Nusselt number. Both parameters are very well approximated by the constant properties model highlighted by relative errors ζ smaller than 1% for almost all simulated cases. A detailed explanation is given in subsection 3.3.4.

3.3.2 Water

When water is simulated, the temperature-dependent changes in density, thermal conductivity and specific heat are negligible compared to the changes in viscosity. An increase in temperature difference decreases the viscosity ratio in Eq. (6) but also increases the velocity gradient at the wall. These effects combine to a slight increase of the friction coefficient. In Fig. 6, the red colors indicate an overestimation of the constant properties model for negative temperature differences and the blue colors and underestimation for positive temperature differences. Regarding the heat transfer, the slight increase in temperature gradient at the wall increases the Nusselt number. Hence, the constant properties model underestimates the Nusselt number for positive temperature differences, and vice versa. Any parts of Fig. 6 in black are outside the property ranges or include a phase change and can not be calculated. The relative error for both friction coefficient and Nusselt number remains small (< 15%) as only temperature differences up to 100 K are possible for liquid water.

3.3.3 Oil

The results for oil are plotted in Fig. 7. The temperature-dependent changes in density, thermal conductivity and specific heat are again small and negligible compared to the changes in viscosity. The explanation for the behavior on the bottom of the plots ($T_{\text{film}} < 390$K) was already given in section 3.2. For higher film temperatures, however, the behavior of the relative errors change, indicated by a decrease in color intensity when moving from bottom to top. The same trend is observed for the Nusselt number with even a change in sign at around $T_{\text{film}} \approx 410$K. As a result, the Nusselt number for oil is very well approximated by the constant properties model for the temperature interval $T_{\text{film}} \in [390\,\text{K};425\,\text{K}]$.

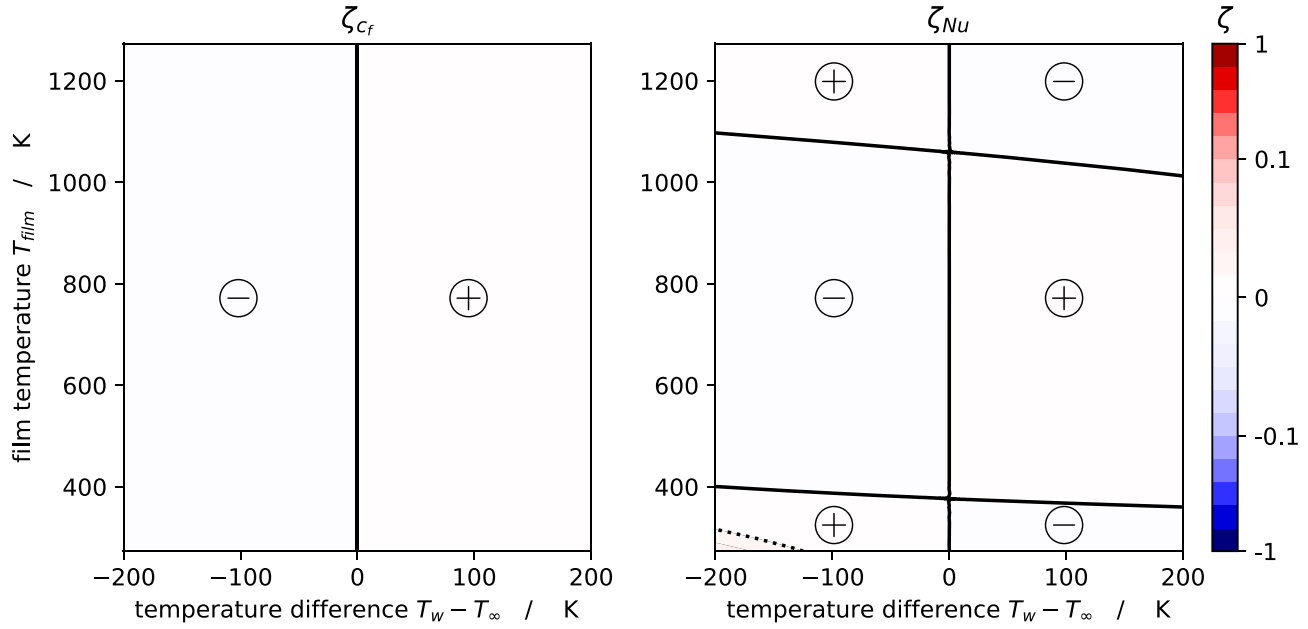

Fig. 5 Relative error of friction coefficient ζ_{c_f} (left) and of Nusselt number ζ_{Nu} (right) for air without dissipation. The black solid and dotted lines indicate a relative error of 0% and 1%, respectively. The signs indicate a small positive or negative relative error

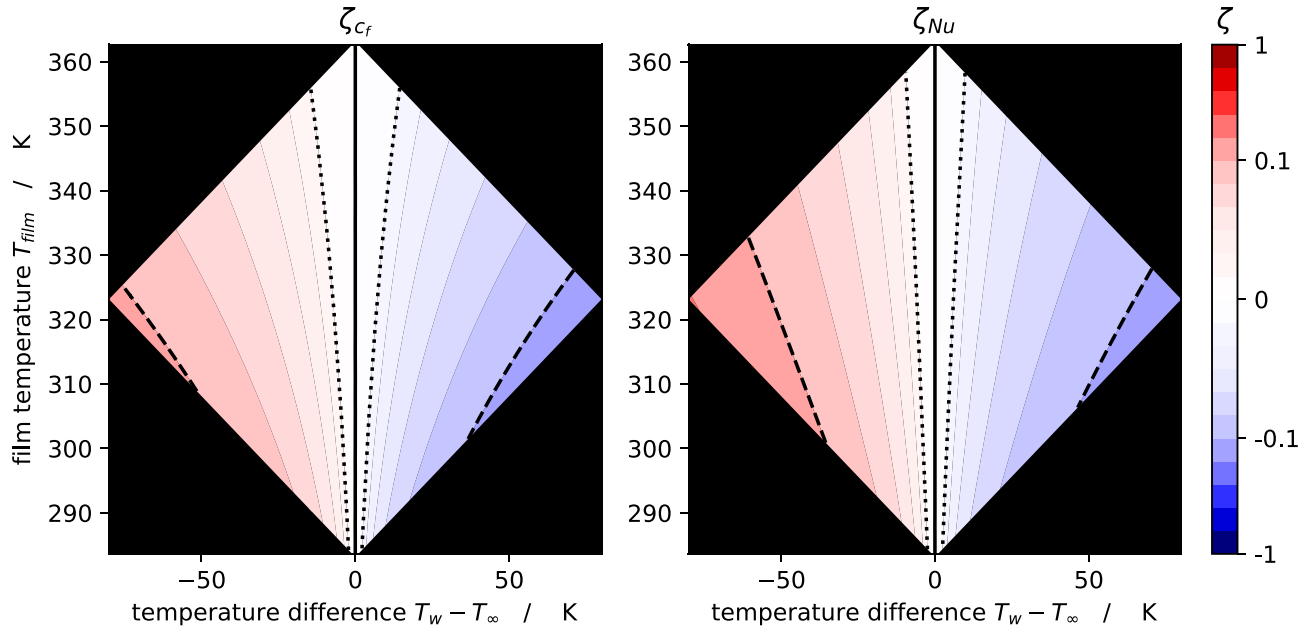

Fig. 6 Relative error of friction coefficient ζ_{c_f} (left) and of Nusselt number ζ_{Nu} (right) for water without dissipation. The black solid, dotted and dashed lines indicate a relative error of 0%, 1% and 10%

3.3.4 Qualitative assessment

All results of Figs. 5, 6 and 7 are summarized qualitatively in Tables 2 and 3. The lowest and highest film temperature for each fluid is evaluated with respect to an increase in temperature difference $T_w - T_\infty$. Diagonal arrows symbolize a slight change while one or more vertical arrows indicate a medium to significant trend. A dash means that the change is below 10% and can be neglected. The input parameters are displayed in the first 3 columns, the terms with respect to the friction coefficient in the 6 columns after that and with respect to the Nusselt number in the last 5 columns. The table enables a deeper understanding of the underlying mechanisms on the fluid flow and heat

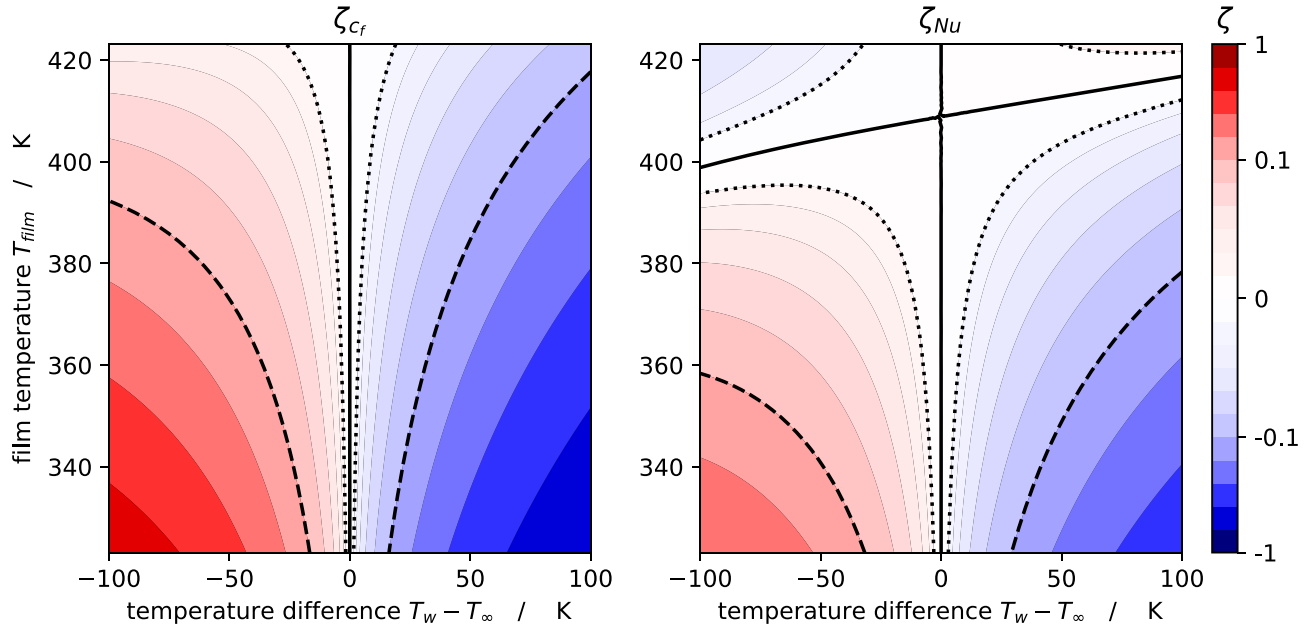

Fig. 7 Relative error of friction coefficient ζ_{c_f} (left) and of Nusselt number ζ_{Nu} (right) for oil without dissipation. The black solid, dotted and dashed lines indicate a relative error of 0%, 1% and 10%, respectively

Table 2 Qualitative evaluation of an increase in temperature difference ($\Delta T \uparrow$) on the fluid flow for different fluids with the variable fluid properties model while neglecting dissipation ($Pr_{\text{film}}\, Ec_{\text{film}} = 0.001$)

fluid	T_{film}	Pr_{film}	$\frac{\rho_w}{\rho_\infty}$	$\frac{\mu_w}{\mu_{\text{film}}}$	$f''(0)$	$c_f\sqrt{Re_x}$	$c_f^*\sqrt{Re_x}$	ζ_{c_f}
air	273	0.67	↓↓	↑	↗	↓	↓	-
air	1273	0.72	↓	↗	-	↘	↘	-
water	293	6.6	-	↓	↑	↗	-	↘
water	353	2.4	-	↓	↑	-	-	-
oil	323	244	↘	↓↓↓	↑↑↑↑	↑↑	↘	↓↓
oil	423	32	↘	↓↓	↑↑	-	↘	↘

transfer when variable fluid properties are accounted for. Since dissipation is being neglected in this section, all terms of the constant properties model are independent of the temperature difference and remain constant. The only dependence on temperature stems from the density ratio explained in section 2.3. Additionally, the adiabatic wall temperature is equal to the free-stream temperature. Therefore, the fraction involving the temperatures always equals 1 and is not included in the table. This yields an inversely proportional relation between Nusselt number and its relative error ζ_{Nu}. Keep in mind that the definition of the relative error allows for negative values and a good approximation of the flow by the constant properties model will only be achieved if the relative error were to be close to zero.

In the case of an air flow, the strong decrease in density with increasing ΔT is partially counteracted by the increase in viscosity and dimensionless velocity gradient at the wall. Overall, this leads to a decrease of the friction coefficient at constant local film Reynolds number for the variable properties model. The friction coefficient of the constant properties model decreases because of the density ratio introduced by the definition of the friction coefficient with the free-stream density. The combination of these effects leads to a very small relative error for the friction coefficient. Regarding the heat transfer of the air flow, the decrease in viscosity is compensated by the increase in thermal conductivity, leading to an almost constant Nusselt number independent of temperature difference.

Regarding a water flow over a flat plate, the decrease in viscosity and the increase in velocity gradient at the wall combine to a slight increase in friction coefficient for increasing temperature difference. The Nusselt number increases slightly because of an increase in temperature gradient at the wall.

The flow behavior of oil is dominated by the decrease in viscosity for an increase in temperature difference. In the case of the high Prandtl number of 244, the velocity gradient at the wall overcompensates this decrease leading to an increasing friction coefficient at a constant film Reynolds number. In the case of the low Prandtl number of 32, these effects offset and the friction coefficient is nearly independent of temperature difference. The slight decrease in density leads to a slightly decreasing relative error ζ_{c_f} with increasing temperature difference. A similar behavior can be seen for the Nusselt number, where the increase in temperature gradient at the wall opposes the decrease in density. The increase in temperature gradient is more dominant for the high Prandtl number case leading to a positive correlation between Nusselt number and temperature difference. However, the effects almost cancel each other out for the low Prandtl number case.

3.4 Variable properties and viscous dissipation

The last effect to be introduced is the dissipation. The last term of Eq. (5) introduces the effect of viscous dissipation into the energy equation. This term will only affect the temperature field if the Prandtl number and the Eckert number were sufficiently large. The Prandtl numbers for water and air are small compared to oil (below 10) over the entire temperature range investigated in this study. The effect of viscous dissipation primarily increases the adiabatic wall temperature. For air for example, a free-stream velocity of 50 m/s increases the adiabatic wall temperature to around 1 K above the free-stream temperature. This temperature increase is proportional

Table 3 Qualitative evaluation of an increase in temperature difference ($\Delta T \uparrow$) on the heat transfer for different fluids with the variable fluid properties model while neglecting dissipation ($Pr_{\text{film}}\, Ec_{\text{film}} = 0.001$)

fluid	T_{film}	Pr_{film}	$\frac{\rho_w}{\rho_{\text{film}}}$	$\frac{k_w}{k_{\text{film}}}$	$g'(0)$	$\frac{Nu}{\sqrt{Re_x}}$	ζ_{Nu}
air	273	0.67	↓	↑	-	-	-
air	1273	0.72	↘	↗	-	-	-
water	293	6.6	-	-	↗	↗	↘
water	353	2.4	-	-	-	-	-
oil	323	244	↘	-	↑	↑	↓
oil	423	32	↘	-	↗	-	-

to the square of the free-stream velocity, following the definition of the recovery factor. For more information, please be referred to White and Majdalani [19]. Dissipation has shown very little effect on the friction coefficient and the Nusselt number as long as $Pr_{\text{film}}|Ec_{\text{film}}| < 1$. However, for oil with Prandtl numbers in the order of 10 to 1000, the mentioned product of Prandtl number times absolute Eckert number can get much bigger than unity. In this case, dissipation effects on the friction coefficient and the Nusselt number cannot be neglected and will be investigated hereafter. The combination of viscous dissipation and variable fluid properties will be investigated for oil at a constant film Prandtl number of $Pr_{\text{film}} = 244$ by varying the temperature difference and the film Eckert number.

The relative error for the friction coefficient as a function of $|Ec_{\text{film}}|$ and ΔT is plotted on the left hand side of Fig. 8. The Eckert number switches signs going from a hot free-stream above a cold wall to a cold free-stream above a hot wall (negative to positive temperature difference). Therefore, the absolute Eckert number was chosen to simplify the plot along with an exponential y-axis to cover a large range of Eckert values. The friction coefficient is mainly influenced by dissipation for $|Ec_{\text{film}}| > 0.1$. The relative error decreases with increasing temperature difference as long as the free-stream is hotter than the wall (negative ΔT). For positive temperature differences, the same trend is only observed for $|Ec_{\text{film}}| < 0.5$. Above this value, the relative error increases with increasing ΔT. The behavior of the relative error of the Nusselt number on the right hand side of Fig. 8 is of a more complex structure. For negative temperature differences, the relative error decreases for all absolute Eckert numbers, but with the slope depending on the Eckert number. For positive temperature differences, the relative error also decreases for $|Ec_{\text{film}}| < 0.1$. Above that value, the relative error is positive for temperature differences up to $\Delta T \approx 30$K and negative for larger temperature differences. The significant influence of viscous dissipation on the fluid flow and heat transfer is clearly shown in Fig. 8. For the chosen Prandtl number of $Pr_{\text{film}} = 244$, viscous dissipation has to be taken into account for the friction coefficient if $|Ec_{\text{film}}| > 0.1$ and for the Nusselt number if $|Ec_{\text{film}}| > 0.01$. These thresholds are dependent on the fluid type and the Prandtl number and have to be verified for every setup and operating condition.

The results of Fig. 8 are summarized in Tables 4 and 5. The structure is chosen as subsection 3.3.4 with the arrows indicating a dependence of the respective terms on an increase in temperature difference. One additional column for the constant properties model is added ($Nu^*/\sqrt{Re_x}$) since the adiabatic wall temperature is no longer equal to the static free-stream temperature. The table is split into positive and negative temperature differences because different dependencies were identified for these two cases. The trends were analyzed for three different absolute Eckert numbers. The first value of 0.001 represents the case that dissipation can be neglected as stated in the previous sections. The evaluation of $|Ec_{\text{film}}| = 0.1$ and 1 are performed to investigate the effect of different strengths of dissipation for a constant film Prandtl number.

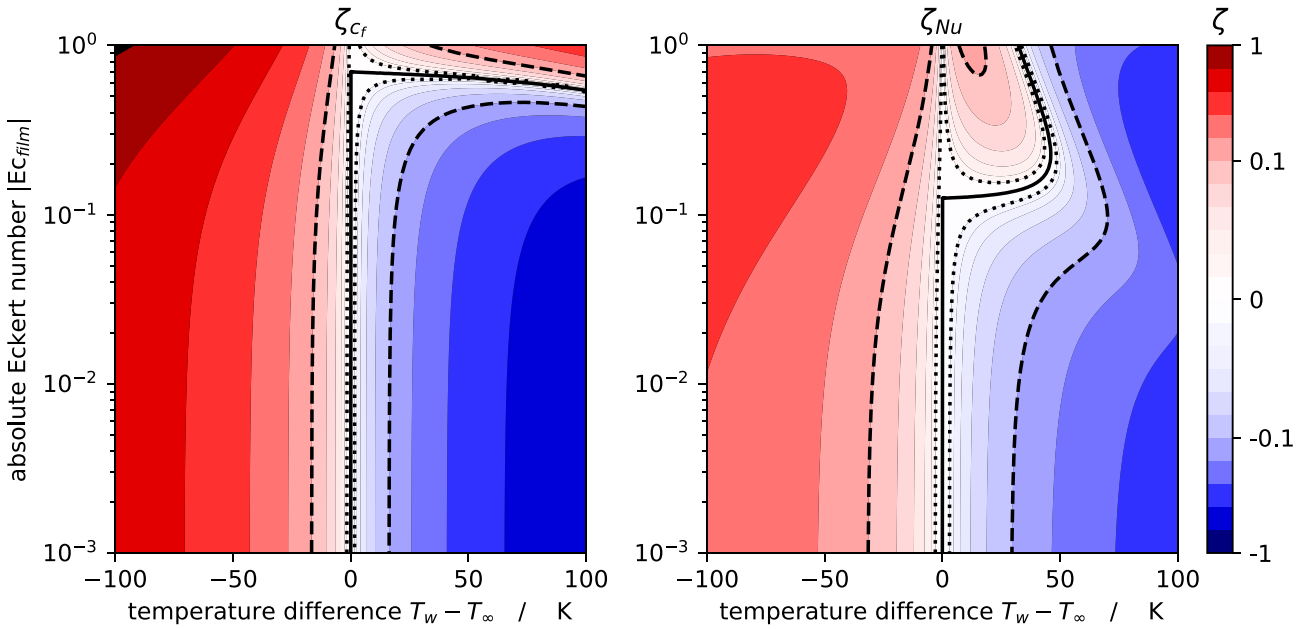

Fig. 8 Relative error of friction coefficient ζ_{c_f} (left) and of Nusselt number ζ_{Nu} (right) for oil at $Pr_{\text{film}} = 244$ (equivalent to $T_{\text{film}} = 323.15$K). The black solid, dotted and dashed lines indicate a relative error of 0%, 1% and 10%, respectively

Table 4 Qualitative evaluation of an increase in temperature difference ($\Delta T \uparrow$) on the fluid flow for oil at $Pr_{\text{film}} = 244$

	Ec_{film}	$\frac{\rho_w}{\rho_\infty}$	$\frac{\mu_w}{\mu_{\text{film}}}$	$f''(0)$	$c_f\sqrt{Re_x}$	ζ_{c_f}
	0.001	↘	↓↓↓	↑↑↑	↑	↓
$\Delta T < 0$	0.1	↘	↓↓↓	↑↑↑	↑	↓
	1	↘	↓↓↓	↑↑↑	↑↑	↓↓
	0.001	↘	↓↓	↑↑↑	↑	↓
$\Delta T > 0$	0.1	↘	↓↓	↑↑↑	↑	↓
	1	↘	↓↓	↑	↓	↑

The results for the case of negligible dissipation has been discussed in the previous section. For a moderate Eckert number of $|Ec_{\text{film}}| \approx 0.1$, the trends for the friction coefficient remain the same whereas for the Nusselt number a change is observed for the constant properties model. The adiabatic wall temperature increases as a result of viscous dissipation heating the boundary layer. For negative temperature differences, this leads to an increase in the denominator of Eq. (7) and subsequently to a decrease in Nusselt number at constant local film Reynolds number $Nu^*/\sqrt{Re_x}$. The opposite effect takes place for positive temperature differences ($T_w > T_\infty$) as the dissipation effect reduces the driving temperature difference for a cold flow over a hot wall. For the variable properties model and negative temperature differences, the increase in adiabatic wall temperature is balanced by the change in temperature gradient at the wall. For positive temperature differences, the effects add up to a positive correlation between Nusselt number and temperature difference.

For a high dissipation case of $|Ec_{\text{film}}| = 1$, the friction coefficient increases even more for negative temperature differences because of an increase in velocity gradient at the wall. For positive temperature differences, the velocity gradient is greatly reduced leading to a negative correlation between the friction coefficient and the temperature difference. Regarding the heat transfer, the effects mentioned in the previous paragraph about the adiabatic wall temperature take also place but in a more pronounced manner. The increase in adiabatic wall temperature dominates all other effects for the constant and variable properties models. This yields a decrease in Nusselt number for negative and an increase for positive temperature differences. The relative error of the Nusselt number exhibits a more complex behavior caused by its definition (Eq. 9). The Nusselt number of the constant properties model is divided by the Nusselt number of the variable properties models. Both of these terms vary differently with increasing temperature difference which explains the behavior of the relative error. For negative temperature differences, the relative error is always positive, meaning the constant properties model overestimates the heat transfer. For positive temperature differences, the trends of the Nusselt numbers for both models are identical but their slopes differ. This leads to the behavior depicted on the right of Fig. 8, where the relative error can be positive or negative depending on the temperature difference and the absolute Eckert number.

3.5 Correlation

In the literature, a correlation already exists for the flow of a compressible gas with variable wall temperature, called the reference temperature concept. The concept is explained in detail in Eckert [20]. The concept states, that the effect of the variable fluid properties can be well approximated as long as they are evaluated at a specific reference temperature. Eckert defines the reference temperature in his study as $T_{\text{ref}} = T_{\text{film}} + 0.22\sqrt{Pr_\infty}u_\infty^2/(2c_{p,\infty})$ [20]. The friction coefficient is approximated by the correlation $c_f = 0.664\sqrt{C_{\text{ref}}}\sqrt{\mu_\infty\rho_{\text{film}}/(\mu_{\text{film}}\rho_\infty)}/\sqrt{Re_x}$. The correlation is adapted to the definition of the dimensionless parameters in this study, which are based on the film temperature instead of the free-stream temperature. The parameter C, also known as the Chapman-Rubesin parameter is defined as $C_{\text{ref}} = \rho_{\text{ref}}\mu_{\text{ref}}/(\rho_\infty\mu_\infty)$. The adiabatic wall temperature evaluates to $T_{\text{aw}} = T_\infty + \sqrt{Pr_{\text{ref}}}\,u_\infty^2/(2c_{p,\infty})$. The Nusselt number correlation, adapted in the same way as before, reads $Nu = 0.332\sqrt{Re_x}\sqrt{C_{\text{ref}}}(Pr_\infty/Pr_{\text{ref}}^{2/3})\sqrt{\mu_{\text{film}}\rho_\infty/(\mu_\infty\rho_{\text{film}})}(k_\infty/k_{\text{film}})$.

Table 5 Qualitative evaluation of an increase in temperature difference ($\Delta T \uparrow$) on the heat transfer for oil at $Pr_{\text{film}} = 244$

	Ec_{film}	$\frac{\rho_w}{\rho_{\text{film}}}$	$\frac{k_w}{k_{\text{film}}}$	$\frac{-\Delta T}{T_w - T_{\text{aw}}}g'(0)$	$\frac{Nu}{\sqrt{Re_x}}$	$\frac{Nu^*}{\sqrt{Re_x}}$	ζ_{Nu}
	0.001	-	-	↗	↗	-	↘
$\Delta T < 0$	0.1	-	-	↗	-	↘	↓
	1	-	-	↓	↓	↓	-/↓
	0.001	-	-	↑	↑	-	↓
$\Delta T > 0$	0.1	-	-	↑	↑	↑	-/↓
	1	-	-	↑↑	↑↑	↑↑	↑ / ↓

When the aforementioned correlations are compared to all the analytical results for air of the variable properties model, an excellent agreement can be observed for the friction coefficient and the Nusselt number. The mean relative error for the friction coefficient is 0.1% with a maximum relative error of 0.7%. Regarding the heat transfer, the mean relative error for the Nusselt number is 1.0% with a maximum relative error of 3.4%. This comparison can also be seen as a validation of the presented methodology.

When the correlations by Eckert are evaluated for water, the mean relative error goes up to 5% for the friction coefficient and 6% for the Nusselt number with maximum relative errors of around 15% for both parameters. The results look even worse for oil (neglecting the dissipation cases) with a mean relative error of 13% and 9% for friction coefficient and Nusselt number, respectively and maximum relative errors as high as 58%. This is why new correlations are derived hereafter to improve accuracy.

For water as fluid, a least square fitting approach yields a very good correlation for the friction coefficient of $c_f = 0.664 C_{\text{film}}^{-0.17} / \sqrt{Re_x}$. The Chapman-Rubesin parameter at film temperature is defined as $C_{\text{film}} = \rho_{\text{film}} \mu_{\text{film}} / (\rho_\infty \mu_\infty)$. This correlation is valid for water at ambient pressure over the entire temperature range of liquid water and for absolute Eckert numbers below 0.1. The maximum relative error for the cases calculated in this study is 3.1%. The Nusselt number is well approximated by the following correlation $Nu = 0.332 \sqrt{Re_x} C_{\text{film}}^{-0.215} Pr_{\text{film}}^{0.33}$. The maximum relative error for the Nusselt number is 3.4%. The adiabatic wall temperature can be approximated with the general approach for the recovery factor, resulting in $T_{\text{aw}} = T_\infty + \sqrt{Pr_{\text{film}}} u_\infty^2 / (2 c_{p,\text{film}})$.

When oil is used as the fluid, a correlation could only be derived for little to no dissipation. The combination of variable properties combined with viscous dissipation leads to non-linear effects, that are difficult to combine into a simple correlation. For a more detailed explanation please be referred to section 3.4. The correlation for the friction coefficient is $c_f = 0.664 (\rho_{\text{film}} / \rho_\infty)^{4.83} \ (\mu_{\text{film}} / \mu_\infty)^{-0.45} / \sqrt{Re_x}$. The maximum relative error of the cases without dissipation is 6.7%. The least square fitting for the Nusselt number yields $Nu = 0.332 \sqrt{Re_x} C_{\text{film}}^{-0.1} Pr_{\text{film}}^{0.34}$ with a maximum relative error of 13%. These correlations are only valid for oil and if $Pr_{\text{film}} |Ec_{\text{film}}| < 1$.

4 Discussion

In the following section the validity of the analytical model is analyzed before implications of the presented results on an application to the superposition method are examined.

4.1 Validity of the model

The assumptions leading up to the analytical model are investigated in this section. The laminar flow assumption is valid up to a certain critical Reynolds number where transition occurs. This criterion can be translated into a length scale over which laminar flow might be present. The current model could be expanded to include turbulent flow with further assumptions as explained by Tsou et al. [21]. An extension including a pressure gradient in x-direction is also possible with certain restrictions as explained by Weigand [12]. Non-Newtonian fluids have been investigated before, e.g. Guedda and Hammouch [22], but are of no relevance for the fluids in this study.

4.2 Application to superposition method

One of the main goals of the analytical investigation is the examination of the applicability of the superposition method for heat transfer measurements. The method is based on the constant properties model and only applicable as long as the error of this model remains small. As shown in section 3.3, the relative error for air is below 1% for almost all operating conditions. The only restrictions are laminar flow and the operating conditions investigated in this study. These restriction could, however, be removed with further improvements to the model as mentioned in section 4.1. For water flows, the relative error of the constant properties model is less than 16% for all operating conditions. A very good approximation (relative error of less than 1%) is observed for small absolute temperature differences of $|\Delta T| < 2\text{K}$ for film temperatures below 300 K increasing to $|\Delta T| < 10\text{K}$ for film temperatures above 350 K. Regarding oil flow, the relative error is highly dependent on the oil film temperature, the temperature difference between wall and free-stream and the Eckert number. A very good approximation is only given for small temperature differences of $|\Delta T| < 3\text{K}$ and for some specific input parameter combinations. One of which is for film temperatures of $T_{\text{film}} \approx 400\text{K}$ as shown in Fig. 7. A reasonably good approximation is found for absolute temperature differences smaller than 30 K without dissipation. Once dissipation affects the temperature field, the differences between the two models discussed in this study are much more complicated to break down, making it difficult to deduce validation restrictions for the constant properties model. Without such restrictions to identify whether the superposition method is valid, the model presented in section 2 should be rerun for the desired fluid properties and operating conditions to check its validity. A possible application of the superposition principle can be found in a previous paper by the authors [23].

5 Conclusions

An analytical model of the Blasius flow is analyzed with respect to the influence of temperature-dependent fluid properties on friction coefficient and Nusselt number. The simplification of a constant properties model is valid for the Nusselt number of a laminar air flow. For a water flow across a flat plate, the differences in friction coefficient and Nusselt number between the two models are about the same and stay below 16%. In the case of an oil flow, the constant properties model is only a valid option for low Prandtl numbers, i.e. high film temperatures, or small temperature differences of a few Kelvin. Dissipation effects on the friction coefficient and the Nusselt number can be neglected for air and water at moderate speeds ($Ec < 0.1$), but have to be included for oil because of its high Prandtl number. The combination of viscous dissipation and variable fluid properties leads to significant deviations for the constant properties model from the variable properties model. Hence, for high Prandtl number fluids, the calculations presented in this study should be repeated for the desired operating conditions to quantify the error of the constant properties model. Once the error deemed acceptable, the superposition method can be applied to quantify the heat transfer. The reference temperature concept by Eckert approximates the flow very well for air, but fails for water and oil. New correlations have been derived for those fluids with better accuracy. These correlations can be used to approximate the friction coefficient and the Nusselt number for all laminar flows of liquid water and for oil flows with temperature differences between wall and free-stream up to 200 K as long as $Pr_{\mathrm{film}}|Ec_{\mathrm{film}}| < 1$.

Acknowledgements The authors would like to thank the German Research Foundation for their funding (DFG project number 437324525).

Author contribution Corina Schwitzke and Hans-Jörg Bauer were responsible for the funding acquisition. All authors contributed to the study conception and design. Model derivation, software development, numerical evaluation and data analysis were performed by Christian Kromer. The first draft of the manuscript was written by Christian Kromer and all authors commented and revised the manuscript. All authors read and approved the final manuscript.

Funding Open Access funding enabled and organized by Projekt DEAL. This work was supported by the German Research Foundation (DFG project number 437324525).

Data availability Raw data were generated at the Institut für Thermische Strömungsmaschinen. Derived data supporting the findings of this study are available from the corresponding author on request.

Declarations

Conflict of interest On behalf of all authors, the corresponding author states that there is no conflict of interest.

References

1. Gritsch M, Baldauf S, Martiny M, Schulz A, Wittig S (1999) The superposition approach to local heat transfer coefficients in high density ratio film cooling flows. In: International Gas Turbine & Aeroengine Congress & Exhibition, pp. 99–16800301048. American Society of Mechanical Engineers, New York. https://doi.org/10.1115/99-GT-168
2. Forth CJP, Loftus PJ, Jones TV (1985) The effect of density ratio on the film-cooling of a flat plate. AGARD-CP-390 Heat Transfer and Cooling in Gas Turbines
3. Blasius H (1907) Grenzschichten in Flüssigkeiten mit kleiner Reibung. Dissertation, Universität Göttingen, Göttingen
4. Hassanien IA (1999) Flow and heat transfer on a continuous flat surface moving in a parallel free stream with variable fluid properties. ZAMM - Zeitschrift für Angewandte Mathematik und Mechanik 79(11):786–792. https://doi.org/10.1002/(SICI)1521-4001(199911)79:11%3C786::AID-ZAMM786%3E3.0
5. Bachok N, Ishak A, Pop I (2012) Boundary layer flow and heat transfer with variable fluid properties on a moving flat plate in a parallel free stream. J Appl Math 2012. https://doi.org/10.1155/2012/372623
6. Pantokratoras A (2008) The Blasius and Sakiadis flow with variable fluid properties. Heat Mass Trans 44(10):1187–1198. https://doi.org/10.1007/s00231-007-0356-2
7. Korpela SA (1985) On the viscous dissipation in the boundary layer of a high Prandtl number fluid in laminar flow over a flat plate. Zeitschrift für angewandte Mathematik und Physik ZAMP 36(4):624–628. https://doi.org/10.1007/BF00945302
8. Fang T (2003) Similarity solutions for a moving-flat plate thermal boundary layer. Acta Mech 163(3):161–172. https://doi.org/10.1007/s00707-003-0004-y
9. Cortell R (2007) Flow and heat transfer in a moving fluid over a moving flat surface. Theor Comput Fluid Dyn 21(6):435–446. https://doi.org/10.1007/s00162-007-0056-z
10. Olanrewaju PO, Gbadeyan JA, Agboola OO, Abah SO (2011) Radiation and viscous dissipation effects for the Blasius and Sakiadis flows with a convective surface boundary condition. Int J Adv Sci Technol 2(4):102–115
11. Anderson JD (2006) Hypersonic and high-temperature gas dynamics, 2nd edn. American Institute of Aeronautics and Astronautics, Reston, Virginia, USA
12. Weigand B (2015) Analytical methods for heat transfer and fluid flow problems. Springer, Heidelberg. https://doi.org/10.1007/978-3-662-46593-6
13. Mureithi EW, Mwaonanji JJ, Makinde OD (2013) On the boundary layer flow over a moving surface in a fluid with temperature-dependent viscosity. Open J Fluid Dyn 135–140. https://doi.org/10.4236/ojfd.2013.32017

14. Khan M, Salahuddin T, Altanji M (2022) A viscously dissipated Blasisus boundary layer flow with variable thermo-physical properties: An entropy generation study. Int Commun Heat Mass Trans 131:105873. https://doi.org/10.1016/j.icheatmasstransfer.2021.105873
15. Andersson HI, Aarseth JB (2007) Sakiadis flow with variable fluid properties revisited. Int J Eng Sci 45(2–8):554–561. https://doi.org/10.1016/j.ijengsci.2007.04.012
16. Zografos AI, Martin WA, Sunderland JE (1987) Equations of properties as a function of temperature for seven fluids. Comput Methods Appl Mech Eng 61(2):177–187. https://doi.org/10.1016/0045-7825(87)90003-X
17. Glahn A (1995) Zweiphasenströmung in Triebwerkslagerkammern - Charakterisierung der Ölfilmströmung und des Wärmeübergangs. Dissertation, Universität Karlsruhe, Karlsruhe
18. Jischa M (1982) Konvektiver Impuls-, Wärme- und Stoffaustausch. Springer, Heidelberg
19. White FM, Majdalani J (2006) Viscous Fluid Flow, vol. 3. McGraw-Hill, New York
20. Eckert ERG (1956) Engineering relations for heat transfer and friction in high-velocity laminar and turbulent boundary-layer flow over surfaces with constant pressure and temperature. Trans Am Soc Mech Eng 78(6):1273–1283. https://doi.org/10.1115/1.4014011
21. Tsou FK, Sparrow EM, Goldstein RJ (1967) Flow and heat transfer in the boundary layer on a continuous moving surface. Int J Heat Mass Trans 10(2):219–235. https://doi.org/10.1016/0017-9310(67)90100-7
22. Guedda M, Hammouch Z (2009) Similarity flow solutions of a non-Newtonian power-law fluid. arXiv preprint arXiv:0904.0315. https://doi.org/10.48550/arXiv.0904.0315
23. Kromer C, Ayan E, Schwitzke C, Bauer H-J (2022) Experimental investigation of the oil jet heat transfer for an aero engine gearbox. In: 25th Conference of the International Society for Air Breathing Engines. https://doi.org/10.5445/IR/1000152758